

# Cycle slip detection, correction and phase leveling of RINEX formatted GPS observables

Shweta Sharma<sup>1</sup>, N. Dashora<sup>2,\*</sup>, P. Galav<sup>1</sup> and R. Pandey<sup>1</sup>

<sup>1</sup>Department of Physics, Mohanlal Sukhadia University, Udaipur 313 001, India

<sup>2</sup>National Atmospheric Research Laboratory, Gadanki 517 112, India

**The implementation of an algorithm to detect and correct the cycle slips in global positioning system (GPS) observables formatted in receiver independent exchange (RINEX) is presented. The cycle slip corrected data has been subjected to phase leveling to determine the total electron content (TEC) for an un-differenced GPS receiver. The efficacy and accuracy of the developed computer codes has been tested for varied ionospheric conditions. It is important to note that this is the first attempt from a low latitude Indian zone for such an implementation.**

**Keywords:** Cycle slip, global positioning system, receiver independent exchange, total electron content.

GLOBAL positioning system (GPS) satellites are being used for ground positioning and navigation purposes using a network of dual frequency GPS receivers. Since the dual frequency phase measurements can be used to derive the ionospheric total electron content (TEC), these receivers, either as a part of a network or individually, are also being used for the study of various ionospheric phenomena and for the assessment of the impact of space weather phenomena on the ionosphere. Considering the wide variety of GPS receivers in use, a common data format became essential to exchange data amongst the user community. Gurtner *et al.*<sup>1</sup> presented the philosophy of such a common data format, called the ‘receiver independent exchange (RINEX)’ format, written in formatted ASCII to guarantee an easy exchange between different computer systems. But to use the RINEX data files is not straightforward as it requires very sophisticated algorithms and computer codes which are either patented or are available only to those who are a part of an international network of GPS receivers, such as the International GNSS Service (IGS). Hence, in spite of the availability of the IGS-RINEX data in the public domain, stand-alone GPS users, like us, could not use this data. This hampers the studies related to phenomena such as the equatorial spread (F) and space weather on a regional or global scale. This has been the sole motivation to develop computer codes to retrieve the RINEX data using the algorithms of Blewitt<sup>2</sup> and others, which are developed

especially for the stand-alone receivers. The algorithm developed by Blewitt<sup>2</sup> was employed in a software package known as GIPSY developed by the Jet Propulsion Laboratory (JPL), USA for geodetic surveying purposes. The complete GIPSY software consists of a set of other algorithms and computer routines in addition to the algorithm and code provided by Blewitt<sup>2</sup>. The source code and algorithms of the GIPSY package are unavailable in the public domain. Moreover, the major task of this software is to provide the precise coordinates of a GPS antenna connected to a stand-alone receiver and not to provide the ionospheric TEC. As a matter of fact, almost all the software packages developed to pre-process/process the GPS data were motivated by geodetic applications and hence provide precise estimation of position. In all such applications, the ionospheric delay (TEC) is considered nothing more than a nuisance parameter. Further in such software, TEC became less significant when the so-called ionosphere free combination<sup>3</sup> of GPS observables from more than one GPS receiver was employed. Till date, a number of methods and packages are available that employ a network of GPS receivers to address the initial ambiguity problem<sup>4</sup> and to correct all excessive delays in the GPS signal that inhibit the precise estimation of position, like BERNESE<sup>5</sup> and GAMIT<sup>6</sup>. Recently, Horvath and Essex<sup>7</sup> have developed software to estimate TEC, wherein they defined the tolerance levels for TEC variation from one epoch to another for detection of the cycle slip. It proved to be a very cumbersome and manifold-multistep method to detect and correct the cycle slips. Similar to the other packages, this software also is not available in the public domain so far; and according to the paper, it is under development. To the best of our knowledge, there is no software available in the public domain that has applicability to ionospheric research – especially for low latitudes. For the ionospheric researcher, TEC is the most significant parameter and therefore, we were prompted to develop the software detailed in this article.

The RINEX data, obtained from GPS receivers, contains primarily the C1 (C/A code pseudo range, in meters, on L1 frequency), P2 (P code pseudo range, in meters, on L2 frequency), L1 (L1 carrier phase, in cycles, on L1 frequency) and L2 (L2 carrier phase, in cycles, on L2 frequency) observables, useful to derive the ionospheric

\*For correspondence. (e-mail: nirvikardashora@gmail.com)

delay in the GPS signal. By the very nature of these code (frequency of code), the code pseudo ranges are noisy but at the same time, these are absolute measurements of the distance from the satellite transmitter to the receiver antenna. But because of the associated noise, these could not be employed directly for the computation of TEC. The carrier phase measurements on the other hand are very precise but cannot be employed directly as these suffer from initial phase ambiguity and cycle slips, as explained later. The initial ambiguity arises due to the fact that the number of cycles associated with the first phase measurement of a satellite pass could not be ascertained. Subsequent phase measurements will have the same associated integer provided the receiver maintains a lock (phase) on the GPS signal. The loss of lock causes integer discontinuity in the phase measurement, which is called a ‘cycle slip’. The term cycle slip detection refers to the detection of the integer jump in the continuous time series data of the carrier phase. The cycle slip can occur on both the L1 and L2 signals. The cycle slip correction or repair refers to the estimation of the exact number of L1 and L2 frequency cycles that comprise the slip, and the actual correction of the phase measurements by these integer estimates.

A minimum cycle slip reception is desirable because maintaining constant track of the phase of the carrier signal from each available GPS satellite is necessary for surveying to centimeter or sub-centimeter precision. Even a loss of signal for as short a time as a nanosecond can cause a cycle slip. Cycle slips degrade the quality and precision of survey data acquired during a flight. Thus, to be able to use the carrier phase data, correction for the cycle slips during a satellite pass is required. Such a cycle slip corrected phase data could then be used for computation of TEC, designated as  $TEC_{\phi}$ .  $TEC_{\phi}$  thus computed is in arbitrary units as it has been derived using the carrier phase data which has inherent initial ambiguity, as discussed earlier. However,  $TEC_{\phi}$  can be used for smoothing of the noisy code pseudo range derived TEC, designated as  $TEC_p$ , resulting in resolution of the initial phase ambiguity.

Hence, to use and analyse the RINEX data for computation of TEC, the main job is to: (i) Detect and remove the cycle slips from the carrier phase data, (ii) Calculate TEC using code pseudo ranges and carrier phases, and (iii) Resolve the initial carrier phase ambiguity.

Various techniques have been developed to detect and correct the cycle slip<sup>2,8-13</sup>. As the present study concerns the data obtained using static, un-differenced GPS receivers, the algorithm proposed by Blewitt<sup>2</sup> has been followed for the detection and removal of the cycle slip. For the resolution of initial phase ambiguity and computation of TEC, the algorithms proposed by Skone<sup>14</sup> and refined by Liu *et al.*<sup>15</sup> have been employed.

### GPS observables

Following Blewitt<sup>2</sup> conservatively, the GPS observables are defined as

$$L_1 = -c\Phi_1 / f_1 = \rho - If_2^2 / (f_1^2 - f_2^2) + \lambda_1 b_1, \quad (1)$$

$$L_2 = -c\Phi_2 / f_2 = \rho - If_1^2 / (f_1^2 - f_2^2) + \lambda_2 b_2, \quad (2)$$

$$P_1 = \rho + If_2^2 / (f_1^2 - f_2^2), \quad (3)$$

$$P_2 = \rho + If_1^2 / (f_1^2 - f_2^2), \quad (4)$$

where  $\Phi_1$  and  $\Phi_2$  are the recorded carrier phases in cycles;  $L_1$  and  $L_2$  the carrier phases expressed as ranges;  $P_1$  and  $P_2$  the P code pseudo ranges;  $c$  the speed of light; the carrier frequencies  $f_1 = 1575.42$  MHz and  $f_2 = 1227.60$  MHz correspond to the wavelengths  $\lambda_1 = 19.0$  cm and  $\lambda_2 = 24.4$  cm respectively. The term  $\rho$  refers to the non-dispersive delay – lumping together the geometric delay, tropospheric delay, clock signatures, selective availability (rapid variations of the 10.23 MHz GPS reference frequency) and any other delay which affects all the data types identically. The term  $I$  is an ionospheric delay parameter;  $b_1$  and  $b_2$  are phase biases which can change spontaneously by an integer value (cycle slips).

### Wide lane and ionospheric combinations

Let a cycle slip have occurred and let the new values of the ambiguities after the cycle slip be  $b'_1$  and  $b'_2$ . Then the cycle slip can be described by the quantities  $\Delta n_1$  and  $\Delta n_2$  (an integer discontinuity) as

$$(\Delta n_1, \Delta n_2) = (b'_1 - b_1, b'_2 - b_2). \quad (5)$$

Cycle slips may occur concurrently and differently on the L1 and L2 channels. So, non-zero values of  $\Delta n_1$  and  $\Delta n_2$  must be independently detectable.

The wide lane phase combination is given by

$$\Phi_{\delta} = \Phi_1 - \Phi_2. \quad (6)$$

The wide lane phase delay can be written as

$$L_{\delta} = -\Phi_{\delta} \lambda_{\delta} = \rho + If_1 f_2 / (f_1^2 - f_2^2) + \lambda_{\delta} b_{\delta}, \quad (7)$$

where the wide lane wavelength is

$$\lambda_{\delta} = c / (f_1 - f_2) = \lambda_1 \lambda_2 / (\lambda_2 - \lambda_1) = 86.2 \text{ cm}, \quad (8)$$

and the wide lane bias is

$$b_{\delta} = (b_1 - b_2). \quad (9)$$

The code pseudo range delay  $P_{\delta}$  is

$$P_{\delta} = (P_1 f_1 + P_2 f_2) / (f_1 + f_2) = \rho + I f_1 f_2 / (f_1^2 - f_2^2). \quad (10)$$

Thus

$$b_{\delta} = (L_{\delta} - P_{\delta}) / \lambda_{\delta}. \quad (11)$$

The ionospheric phase combination  $L_I$  is

$$\begin{aligned} L_I &= L_1 - L_2 \\ &= I + \lambda_1 b_1 - \lambda_2 b_2 \\ &= I + \lambda_1 (b_1 - b_2) + (\lambda_1 - \lambda_2) b_2 \\ &= I + \lambda_1 b_{\delta} - \lambda_1 b_2, \end{aligned} \quad (12)$$

where the ionospheric wavelength or the narrow lane wavelength is

$$\lambda_I = \lambda_2 - \lambda_1 = 5.4 \text{ cm}. \quad (13)$$

The corresponding pseudo range combination is

$$P_I = P_2 - P_1 = I. \quad (14)$$

### Cycle slip detection

According to the algorithm of Blewitt<sup>2</sup>, the wide lane bias is estimated independently at every data epoch. The mean value of  $b_{\delta}$ ,  $\langle b_{\delta} \rangle$  and the RMS scatter ( $\sigma$ ) are calculated by the recursive formulae

$$\langle b_{\delta} \rangle_i = \langle b_{\delta} \rangle_{i-1} + (b_{\delta i} - \langle b_{\delta} \rangle_{i-1}) / i \quad (15)$$

$$\sigma_i^2 = \sigma_{i-1}^2 + \{(b_{\delta i} - \langle b_{\delta} \rangle_{i-1})^2 - \sigma_{i-1}^2\}. \quad (16)$$

The algorithm demands that the subsequent epoch estimates,  $b_{\delta i+1}$  have to be within  $4\sigma_i$  of the running mean  $\langle b_{\delta} \rangle_i$ . If a single value of  $b_{\delta i}$  is beyond the aforementioned limit, it is called an outlier and the specific data epoch is deleted. If any two consecutive values of  $b_{\delta}$  at two consecutive epochs are outside this limit, and if these two values are lying within one cycle, then it is considered as a cycle slip at the epoch  $i$ . Beginning with these two points, a new average is started and continues until a potential cycle slip is again encountered. Thus, the positions of the cycle slips presented in wide lane phase delay  $L_{\delta}$  have been obtained.

This process has been exemplified in Figure 1 for a GPS satellite PRN 4 over Udaipur on 14 December 2005, an international geomagnetic quiet day. The top two panels of Figure 1 show plots of raw carrier phase measure-

ments,  $L_1$  and  $L_2$ . While the  $L_1$  measurements are continuous, discontinuity in  $L_2$  at epochs 93 and 152 is obvious. Thus, in this example, a cycle slip has occurred at epochs 93 and 152. But, the process discussed earlier does not check the discontinuities in  $L_1/L_2$  individually; rather, it does so in the wide lane phase delay  $L_{\delta}$ , so that the discontinuities in  $L_1$  or  $L_2$  or both are determined. Hence, the process has led to the detection of cycle slips in the wide lane phase delay  $L_{\delta}$ , at epoch number 93 and 152 respectively, as shown in the bottom panel of Figure 1. Thus, the wide lane phase delay comprises segments, drawn with different colours and marked 1 through 3. These are termed as the different phase connected arcs.

### Cycle slip correction

Cycle slip correction requires removing the discontinuities in different phase connected arcs and producing a continuous curve.

After the successful detection of all cycle slips in a given pass of a satellite, the integer ambiguities  $\Delta n_1$  and  $\Delta n_2$  in  $L_1$  and  $L_2$  carrier phase measurements, for each phase connected arc, have to be found out separately in order to connect all phase connected arcs. For this, the first step is to estimate the integer discontinuity  $\Delta n_{\delta}$  in the wide lane phase delay  $L_{\delta}$ .

$$\Delta n_{\delta} = b'_{\delta} - b_{\delta}. \quad (17)$$

The scheme adopted by us requires computation of the wide lane correction between two consecutive phase connected arcs. Simultaneously, the standard error in  $b_{\delta}$  for each phase connected arc is computed separately. The arc with minimum standard error is chosen as the reference arc, with respect to which phase leveling amongst the phase connected arcs is to be attempted.

Then, using the ionospheric phase correction method as given by Blewitt<sup>2</sup>, the values of integer discontinuity in  $L_2$  carrier phase have been calculated. Using these two integer values, viz.  $\Delta n_{\delta}$  and  $\Delta n_2$ , the value of  $\Delta n_1$  has been computed by the formula

$$\Delta n_{\delta} = \Delta n_1 - \Delta n_2. \quad (18)$$

Using the values of  $\Delta n_1$  and  $\Delta n_2$ , the discontinuities, if any, in  $L_1$ ,  $L_2$  and  $L_{\delta}$  have been corrected (Figure 2).

The software developed for cycle slip detection and correction was tested for 8568, 11,148 and 9410 passes of GPS satellites viewed from Udaipur for 2005, 2007 and 2009 respectively under varied solar activity levels. The results for this test are given in Figure 3 which shows the percentage detection to be 100 and correction of the detected slips to be 84.77, 85.44 and 86.86 for the aforementioned years. The uncorrected cycle slips correspond to the part of the pass that is either in the beginning or at

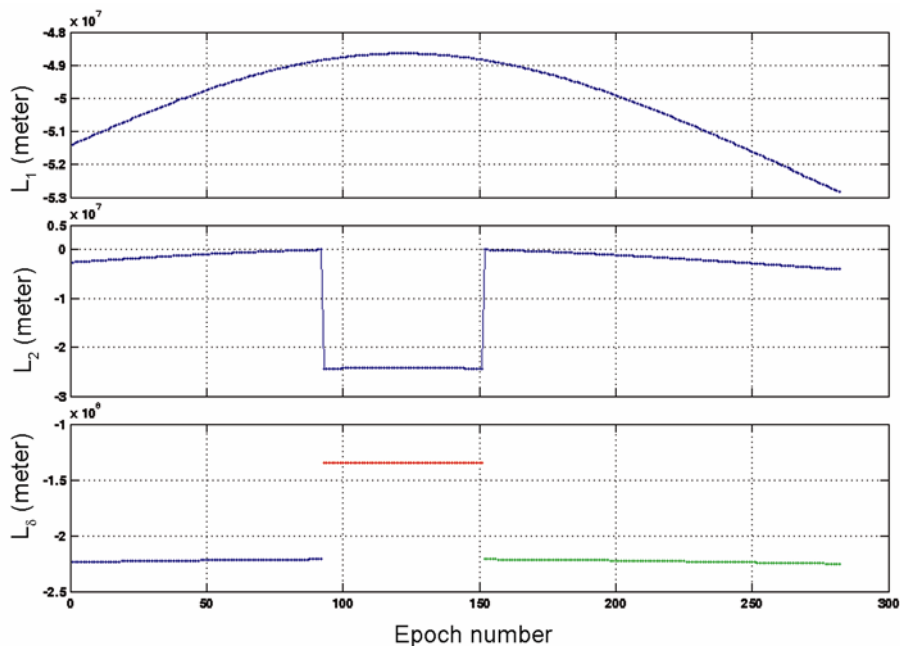


**Figure 1.** The raw carrier phase measurements  $L_1$  and  $L_2$  (top two panels) and the computed wide lane phase delay  $L_\delta$  (bottom most panel) revealing the cycle slips at epoch 93 and 152 in  $L_2$  and  $L_\delta$  for GPS satellite PRN 4 on 14 December 2005 over Udaipur.

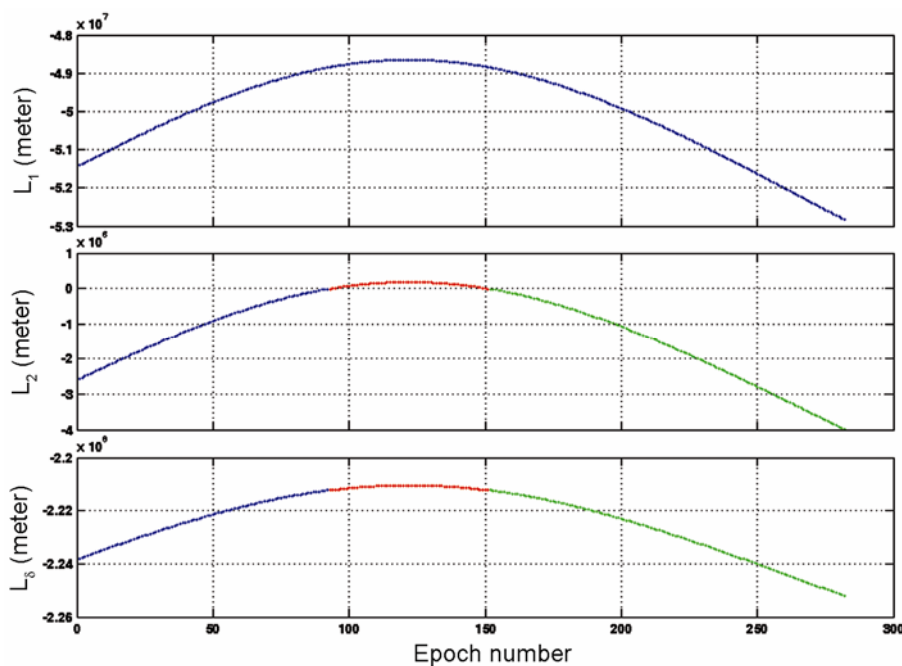


**Figure 2.** The cycle slip corrected carrier phases  $L_1$  and  $L_2$  (top two panels) and wide lane phase delay  $L_\delta$  (bottom most panel) for GPS satellite PRN 4 on 14 December 2005 over Udaipur. Discontinuous arcs of  $L_2$  and  $L_\delta$  of Figure 1 have been corrected and are shown as a single phase connected arc. Different colours in the single arc correspond to the original discontinuous arcs.

the end of the pass when the elevation angle is less than  $20^\circ$  or within the first 15 points of the pass. Blewitt<sup>2</sup> had also opined that at least 15 points should elapse for the algorithm to be effective and our results indicate a similar limitation of the algorithm.

### Calculation of TEC from GPS observables

The detection and correction of cycle slips facilitate the availability of continuous segments of  $L_1$  and  $L_2$ , which

are employed for the computation of  $TEC_\phi$ . The true  $TEC_\phi$  is given by

$$TEC_\phi = -f_1^2 f_2^2 [(L_1 - L_2) - \lambda_1 N_1 + \lambda_2 N_2 - b_r - b_s] / [40.3 \times 10^{16} (f_1^2 - f_2^2)]. \quad (19)$$

Here  $TEC_\phi$  is in TECU,  $b_r$  and  $b_s$  are GPS receiver and satellite inter-frequency biases for carrier phase measurements respectively, and  $N_1$  and  $N_2$  are the integer phase ambiguities for  $L_1$  and  $L_2$ .

Using the code pseudo measurements  $P_1$  and  $P_2$ ,  $TEC_p$  has been calculated using

$$TEC_p = -f_1^2 f_2^2 [(P_1 - P_2) - B_r - B_s] / [40.3 \times 10^{16} (f_1^2 - f_2^2)]. \quad (20)$$

Here  $TEC_p$  is in TECU ( $1 \text{ TECU} = 10^{16} \text{ electrons/m}^2$ );  $B_r$  and  $B_s$  are GPS receiver and satellite inter-frequency biases respectively, for the code measurements.

While describing the eqs (1)–(4), we mentioned that  $\rho$  represents the lump estimate of all other delays, the multipath assumed to be included in  $\rho$ . Blewitt<sup>2</sup> has noted that multipath is a site-specific error in the GPS signal and cannot be corrected in the post-processing mode; it remains as an unresolved differential error in TEC. Similar results were obtained in the analysis by Ciralo *et al.*<sup>16</sup>. Thus, we minimized the effect of multipath in our data by raising the height of the antenna using a mast of about 30 feet over and above the roof-top of the Department of Physics building, Mohanlal Sukhadia University (MLSU), Udaipur. Moreover, the antenna (NovAtel's GPS702) attached with the GPS receiver uses a special technology to combat multipath. Thus, the multipath in our data is minimized and its effect on TEC, if any,

remains well below 5–7° elevation angles in all directions. There is no impact of multipath above this elevation angle and hence does not cause any concern for our software. Also, it shall be noted that multipath affects the code pseudorange 100 times more than the carrier phase<sup>17</sup>, and since we use the leveled carrier phase observations as the estimated TEC, multipath effects are at minimal level.

As discussed earlier,  $TEC_p$  is precise but noisy whereas  $TEC_\phi$  is smooth but suffers from inherent initial ambiguity. So, the leveling of  $TEC_\phi$  by  $TEC_p$  or the smoothing of  $TEC_p$  by  $TEC_\phi$  could be done to derive a precise and smooth TEC. For the smoothing of  $TEC_p$ , various methods have been developed<sup>14,15,18–24</sup>.

In the present work, the method discussed by Liu *et al.*<sup>15</sup> has been used for the smoothing of  $TEC_p$ . In this, the smoothed differences for consecutive measurements,  $\delta(TEC_k)_{sm}$ , have been calculated using the recursive formula

$$\delta(TEC_k)_{sm} = \{[(k-1)\delta(TEC_{k-1})_{sm}] + \{(TEC_p)_k - (TEC_\phi)_k\}\} / k, \quad (21)$$

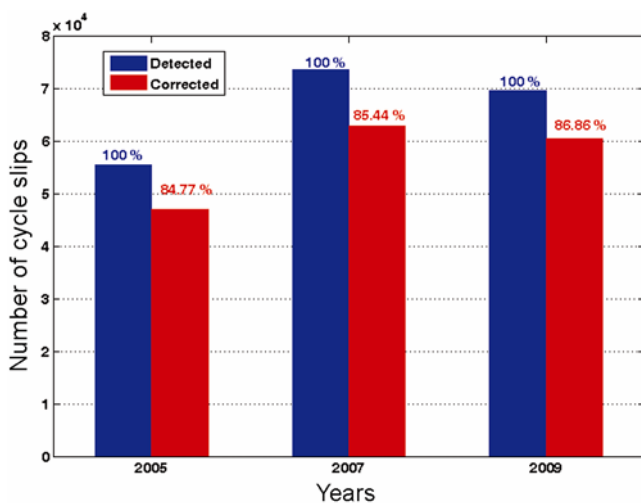
where  $k$  is the epoch number at any given instant.

This smoothed offset  $\delta(TEC_k)_{sm}$  is then added up to the  $TEC_\phi$  to obtain the smoothed or leveled TEC at each epoch,

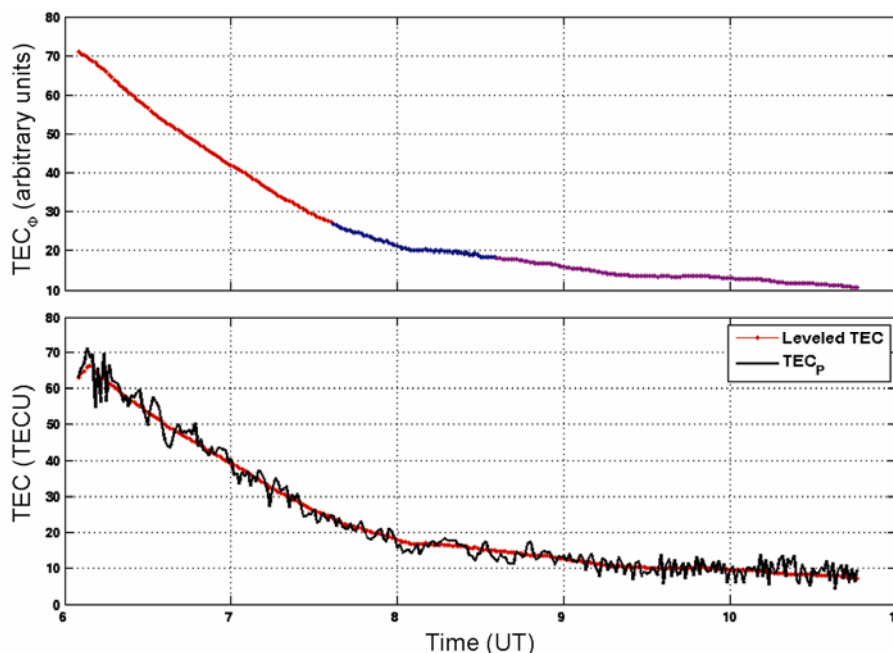
$$(TEC_k)_{sm} = (TEC_\phi)_k + \delta(TEC_k)_{sm}. \quad (22)$$

Implementation of the procedure given by Liu *et al.*<sup>10</sup> is demonstrated in Figure 4 where the cycle slip corrected  $TEC_\phi$ , with different colours for the various phase connected arcs, is shown in the upper panel. The noisy  $TEC_p$ , drawn in black, has been shown in the lower panel of Figure 4. The leveled TEC, obtained through the procedure discussed earlier, is plotted along with the  $TEC_p$ . It can be seen from Figure 4 that the leveled TEC faithfully represents the trend in  $TEC_p$ . Thus, the efficacy of the procedure is established. To quantitatively represent the improvement in accuracy of TEC due to leveling, we analysed all the passes used to generate Figure 3. We derived the standard deviation ( $\sigma$ ) of  $TEC_p$  for a running window of 5 min. Then, we estimated the percentage accuracy of the phase leveled TEC for a given pass if it remains within  $\pm 1 \sigma$  and  $\pm 2 \sigma$  of the  $TEC_p$ . The results of this accuracy analysis are shown in Figure 5 for 2005, 2007 and 2009 TEC data. It is obvious that the leveled TEC remains more than 89% of the time for  $\pm 1 \sigma$  and more than 96% for  $\pm 2 \sigma$  of the  $TEC_p$ . Obviously, the accuracy and precision of the leveled TEC are highly enhanced.

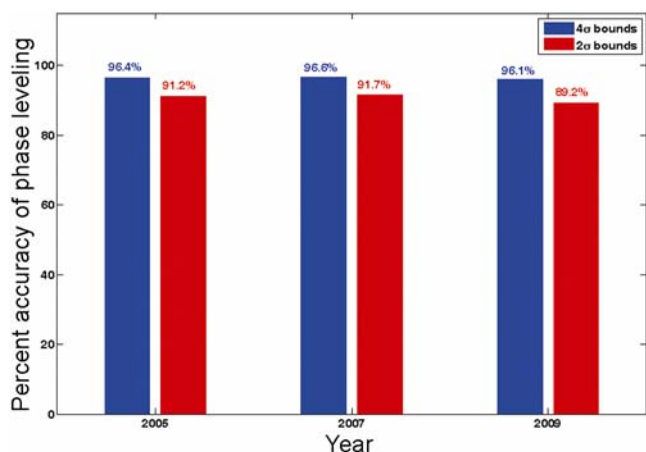
The leveled TEC computed through the above mentioned procedure is the TEC value between a satellite-receiver pair. Thus, this is the slant TEC as the elevation angle of a GPS satellite changes continuously. The credibility of



**Figure 3.** Percentage detection and correction of cycle slips for 2005, 2007 and 2009 for data from Udaipur.

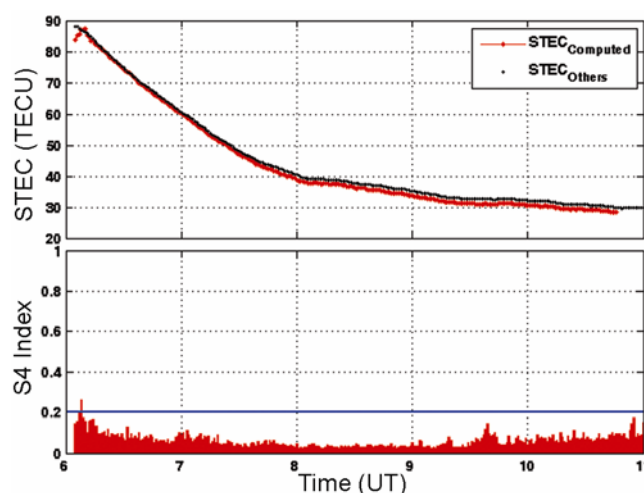


**Figure 4.** An example of TEC leveling for data of GPS satellite PRN 4 on 14 December 2005.  $TEC_{\phi}$  (carrier phase derived TEC) variations, depicted with three different colours for different phase connected arcs, are shown in the upper panel. Due to inherent initial ambiguity, the units are arbitrary. Noisy  $TEC_P$  (code derived TEC), shown in black, has been leveled using  $TEC_{\phi}$  in red in the lower panel.



**Figure 5.** Percentage accuracy of the phase leveling procedure for 2005, 2007 and 2009 for TEC over Udaipur.

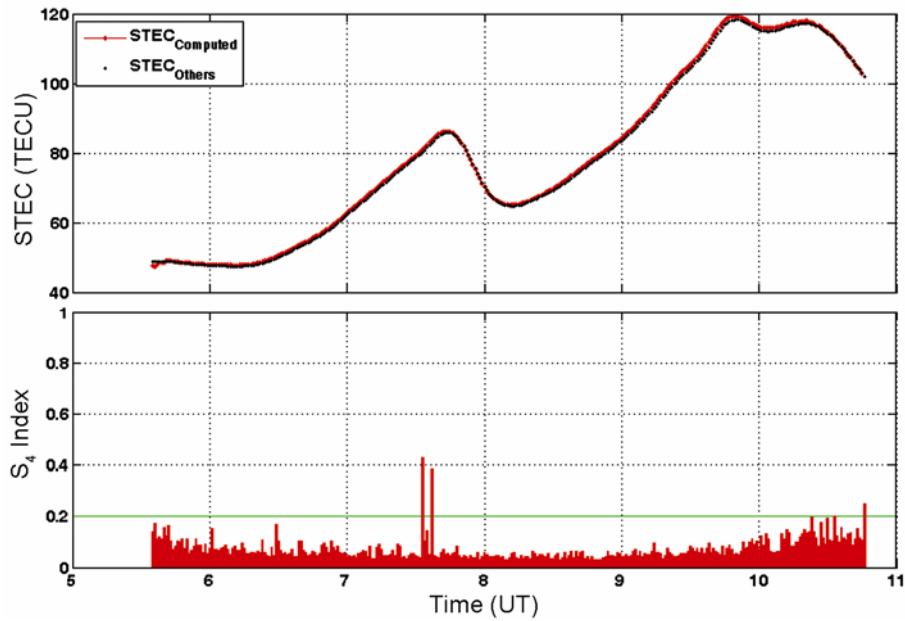
this procedure to derive the (slant) TEC cannot be established until its results are compared with those from an established procedure. The GPS receiver GSV4004A (manufacturer – M/s GPS Silicon Valley; name of the receiver – GSV4004A ‘GPS Ionospheric Scintillation and TEC Monitor’), installed since 2004 at Udaipur, is equipped with firmware to compute the slant TEC. Here, we compare the results on slant TEC obtained with the procedure detailed in this article with those provided by the firmware built in the GSV4004A receiver. For this, three specific cases are considered, viz. a quiet day, a geomagnetically disturbed day and a high scintillation activity day.



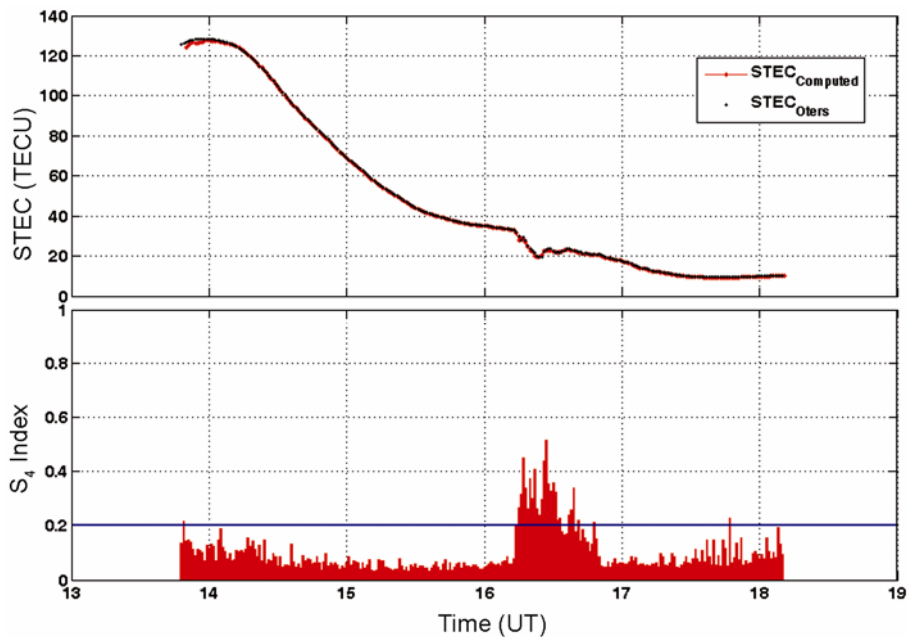
**Figure 6.** Comparison of slant TEC computed using the present procedure (red) and using the software of GSV4004A (black) in the top panel for GPS satellite PRN 4 on 14 December 2005 over Udaipur. One-to-one correspondence is obvious. Low ionospheric scintillation index ( $S_4$ ) in the bottom panel implies a no scintillation quiet day.

Figure 6 gives such a comparison of the slant TEC for a quiet day, 14 December 2005 for the GPS satellite PRN 4 over Udaipur. The slant TEC computed using the software of GSV4004A is plotted in black in the top panel of Figure 6. The curve in red corresponds to the one computed using the present procedure. An excellent agreement between the two is obvious. In the lower panel, the scintillation index  $S_4$  has been plotted.

The scintillation index is defined as the square root of the normalized variance of intensity. The time interval



**Figure 7.** Same as Figure 6 but on a geomagnetically disturbed day, 15 May 2005, for GPS satellite PRN 15 over Udaipur. High value of  $S_4$  after 07:30 UT is an artefact and should be ignored.



**Figure 8.** Same as Figure 6, but on a high scintillation night of 28 October 2004, for GPS satellite PRN 10 over Udaipur.

over which  $S_4$  is calculated is one minute with 50 Hz sampling at  $f_1$  frequency of GPS signal. A low value of  $S_4$  ( $<0.2$ ) implies insignificant scintillations on a quiet day.

In Figure 7, a similar comparison is made for a geomagnetically disturbed day, 15 May 2005, for the GPS satellite PRN 15 over Udaipur. Again, an excellent agreement is seen between the TEC curves obtained using the two approaches.

As a last comparison exercise, a case when the ionospheric TEC was highly variable, as evidenced by short duration fluctuations in the (slant) TEC, has been considered and presented in Figure 8 for the GPS satellite PRN 10 on 28 October 2004. From the lower panel of Figure 8, very high scintillation activity for this case is seen. A very good agreement between the two cases is again obtained, proving the efficacy of the procedure presented here vis-à-vis the standard procedure.



**Figure 9.** Set-up of experiment in Atmospheric and Ionospheric Laboratory at the Department of Physics, Mohanlal Sukhadia University, Udaipur.

The experimental set-up of the receiver GSV4004A has been shown in Figure 9. The control PC is a Pentium IV machine with Microsoft Windows XP operating system. The receiver is controlled by the software provided by the manufacturer. The antenna is installed on the roof-top of the building and the running length of the cable from the antenna to the receiver is 30 m, as provided by the manufacturer.

The suitability and accuracy of the present procedure is established for a variety of ionospheric conditions likely to be encountered in ionospheric research. Hence, the procedure could be used with full confidence for the retrieval of TEC data available in the public domain in RINEX format.

1. Gurtner, W., Mader, G. and MacArthur, D., A common exchange format for GPS data. In Proceedings of the Fifth International Geodetic Symposium on Satellite Systems, Las Cruces, New Mexico, 1989, p. 917.
2. Blewitt, G., An automatic editing algorithm for GPS data. *Geophys. Res. Lett.*, 1990, **17**(3), 199–202.
3. Hoffman-Wellenhof, B., Lichtegger, H. and Collins, J., *GPS: Theory and Practice*, Springer-Verlag, New York, 5th edn, 2001.
4. Sardon, E., Rius, A. and Zarraoa, N., Estimation of the transmitter and receiver differential biases and the ionospheric total electron content from Global Positioning System observations. *Radio Sci.*, 1994, **29**(3), 577–586.
5. Beutler, G. *et al.*, Bernese GPS Software Version 4.2, Astronomical Institute, University of Bern, Bern, 2001.
6. Herring, T. A., King, R. W. and McClusky, S. C., *GPS Analysis at MIT – Release 10.35*, Massachusetts Institute of Technology, USA, 2009.
7. Horvath, I. and Crozier, S., Software developed for obtaining GPS-derived total electron content values. *Radio Sci.*, 2007, **42**, 1–20; doi:10.1029/2006RS003452.
8. Bastos, L. and Landau, H., Fixing cycle slips in dual-frequency kinematic GPS-applications using Kalman filtering. *Manuscripta Geodaetica*, 1998, **13**(4), 249–256.

9. Seeber, G., *Satellite Geodesy*, Walter de Gruyter and Co., Berlin, 1993, p. 531.
10. Collin, F. and Warnant, R., Application of wavelet transform for GPS cycle slip correction and Comparison with Kalman Filter. *Manuscripta Geodetica*, 1995, **20**, 161–172.
11. Gao, Y., Heroux, P., Liao, X., Lahaye, F., Beck, N. and Olynik, M., GPS instrumental bias between receivers. ION GPS Annual Meeting, Cambridge, MA, 1999, p. 55.
12. Bisnath, S. B., Efficient, automated cycle-slip correction of dual-frequency kinematic GPS data. In Proceedings of ION GPS 2000, Salt Lake City, Utah, 2000, pp. 145–154.
13. Bisnath, S. B., Kim, D. and Langley, R. B., A new approach to an old problem: carrier-phase cycle slips. *GPS World*, 2001, **12**(5), 46–51.
14. Skone, S., Wide area ionospheric grid modeling in the auroral region. PhD thesis, Department of Geomatics Engineering, The University of Calgary, Canada, 1998.
15. Liu, Z. Z., Gao, Y. and Skone, S., A study of smoothed TEC precision inferred from GPS measurements. *Earth Planets Space*, 2005, **57**, 999–1007.
16. Ciraolo, L., Azpilicueta, F., Brunini, C., Meza, A. and Radicella, S. M., Calibration errors on experimental slant total electron content (TEC) determined with GPS. *J. Geodesy*, 2007, **81**, 111–120.
17. Braasch, M., Multi-path effects. In *Global Positioning System: Theory and Applications, Vol 1. Progress in Astronautics and Aeronautics* (eds Parkinson, B. W. and Spilker, J. J.), American Institute of Aeronautics and Astronautics, Washington, DC, 1996, pp. 547–568.
18. Hatch, R., The synergism of GPS code and carrier measurements. In Proceedings of the Third International Geodetic Symposium on Satellite Doppler Positioning, Physical Science Laboratory, New Mexico State University, USA, 1982, vol. II, pp. 1213–1232.
19. Lachapelle, G., GPS-current capabilities and prospects for multi-purpose offshore surveying. In Proceedings of the FIG-XVIII International Congress, Toronto, Lighthouse, 1986, vol. 34, pp. 18–22.
20. Jin, X. X., Theory of carrier adjusted DGPS positioning approach and some experimental results. PhD thesis, Delft University Press, Delft, 1996.
21. Liu, Z. Z. and Gao, Y., Ionospheric tomography using GPS measurements. In Proceedings of the International Symposium on Kinematic Systems in Geodesy, Geomatics and Navigation, Banff, Alberta, Canada, 2001.
22. Gao, Y., Liao, X. and Liu, Z. Z., Ionosphere modeling using carrier smoothed ionosphere observations from a regional GPS network. *Geomatica*, 2002, **56**(2), 97–106.
23. Gao, Y. and Liu, Z., Precise ionosphere modelling using regional GPS network data. *J. Global Position. System*, 2002, **1**(1), 18–24.
24. Liu, Z. Z., Ionosphere tomographic modeling and applications using Global Positioning System (GPS) measurements. PhD thesis, Department of Geomatics Engineering, The University of Calgary, Canada, 2004, p. 304.

**ACKNOWLEDGEMENTS.** The GSV4004A GPS receiver at Udaipur was purchased through the grants from UGC, New Delhi under the DRS-SAP and X plan. This work is partially supported under the ISRO-RESPOND program. S.S. thanks the UGC for the UGC-NET-SRF fellowship.

Received 8 March 2010; revised accepted 29 October 2010